

# Generation and radiation of ultra-wideband electromagnetic pulses with high stability and effective potential

A.M. EFREMOV, V.I. KOSHELEV, B.M. KOVALCHUK, V.V. PLISKO, AND K.N. SUKHUSHIN

Institute of High Current Electronics SB RAS, Tomsk, Russia

(RECEIVED 24 March 2014; ACCEPTED 27 April 2014)

## Abstract

An ultra-wideband radiation source based on the excitation of a 64-element array of combined antennas by a generator of bipolar voltage pulses with the length of 1 ns, amplitude of 200 kV and pulse repetition rate of 100 Hz has been designed and studied. The peak power of the voltage pulse was 3.2 GW. The effective potential of the ultra-wideband source radiation reached 4.3 MV.

**Keywords:** Bipolar pulse former; Effective potential of radiation; High-power ultra-wideband radiation; Multi-channel power divider; Multi-element antenna array

## 1. INTRODUCTION

Research and development of the sources of ultra-wideband (UWB) electromagnetic pulses have been intensively conducted already for over 20 years (Baum & Farr, 1993; Koshelev *et al.*, 1997; Agee *et al.*, 1998). The main parameter characterizing the sources of UWB radiation is the effective potential (or figure-of-merit, Agee *et al.*, 1998), defined as the product of the peak electric-field strength  $E_p$  by the distance  $r$  in the far-field zone ( $rE_p$ ). Among the large number of research, we will mention only two directions which allowed creating the sources of UWB radiation with a multi-megavolt effective potential.

The first direction is related to the use of radiators of the impulse radiating antenna type with a large-diameter reflector in UWB sources (Giri *et al.*, 1997; Sabath *et al.*, 2002; Baum *et al.*, 2004). In the course of this research, radiation pulses of ~100 ps length with an effective potential of 5.4 MV were obtained at the JOLT setup (Baum *et al.*, 2004). UWB radiation sources of this type are simple in design but have low energy efficiency due to the use of a voltage pulse with a short rise time and long pulse decay.

The second direction which is developed in this work is related to the use of multi-element arrays excited with a bipolar voltage pulse through a power divider. Within the framework of this research, a combined antenna (CA) with an

extended bandwidth (Koshelev *et al.*, 2001; Andreev *et al.*, 2005) and a bipolar pulse former (BPF) (Andreev *et al.*, 2003) were suggested. A line of high-power UWB radiation sources based on the excitation of 16-element arrays with bipolar voltage pulses of the length ranging from 0.2 to 2 ns (Gubanov *et al.*, 2005; Efremov *et al.*, 2007; 2011; Andreev *et al.*, 2011) was created, and radiation pulses with the effective potential ranging from 0.4 to 1.7 MV were obtained at a pulse repetition rate of 100 Hz. A feeder system, including in series a wave transformer of 50  $\Omega$ /3.125  $\Omega$  and a 16-channel power divider, was used in all these UWB sources. This feeder system limited the number of the elements in the array.

A new feeder system in which a wave transformer and a power divider were combined into a unified device was suggested for a 64-element array (Koshelev *et al.*, 2010). In the UWB source with a 64-element array excited with a bipolar voltage pulse of the length  $\tau_p = 1$  ns and amplitude of 200 kV at the pulse repetition rate of 100 Hz, radiation pulses with the effective potential of 2.8 MV (Koshelev *et al.*, 2008) were obtained. However, radiation stability was low, which was caused by the electrical breakdowns in the BPF made on the basis of radial lines. Additionally, transformer oil was used for electrical insulation of coaxial lines of the feeder system resulting in large energy losses.

The goal of this work is to improve the stability and the effective potential of radiation of the UWB source with a 64-element array by creating a new BPF and reducing energy losses in the feeder system.

Address correspondence and reprint requests to: V.I. Koshelev, Institute of High Current Electronics SB RAS, 2/3 Akademicheskoy Ave., Tomsk 634055, Russia. E-mail: [koshelev@lhfe.hcei.tsc.ru](mailto:koshelev@lhfe.hcei.tsc.ru)

## 2. DESIGN OF THE SOURCE

The main components of the source are the following: a monopolar pulse generator, a bipolar pulse former, a power divider, and a transmitting UWB antenna array. Figure 1 presents a physical configuration of the source.

A monopolar pulse generator is based on the coaxial line with a built-in Tesla transformer of the SINUS-200 type (Mesyats *et al.*, 2003). A distinctive feature of this generator is a more high-voltage primary circuit of the Tesla transformer. A monopolar voltage pulse is applied from the generator to the BPF input. The BPF converts a monopolar pulse into a bipolar one of the length  $\tau_p = 1$  ns and amplitude of 200 kV.

The bipolar pulse with the peak power of 3.2 GW enters the input of the power divider by a coaxial line with the wave impedance of  $12.5 \Omega$  and is divided into 64 channels. The pulses synchronously enter the inputs of the array ( $8 \times 8$ ) elements by the feeder lines with the wave impedance of  $50 \Omega$ . The array elements are CA optimized for bipolar voltage pulses of the length  $\tau_p = 1$  ns. The antennas with a transverse dimension of  $15 \times 15$  cm are placed on a metal plate with a period  $d = 18$  cm in two perpendicular directions. The transverse array size is  $141 \times 141$  cm. Radiation pulses from all elements of the array are added synchronously in the far-field zone, forming a wave beam with a pattern full width at half maximum by the peak power of  $10^\circ$ .

The design details of the UWB source and its operation modes are presented below.

## 3. BIPOLAR PULSE GENERATOR

A bipolar voltage pulse generator consists of a monopolar pulse generator, a preliminary sharpening stage, and a BPF. In the circuit diagram of the bipolar voltage pulse generator shown in Figure 2, the monopolar pulse generator is presented by an output forming line  $FL_0$  with the wave impedance of  $28.3 \Omega$  and electric length of 3.9 ns and by a gas gap switch  $S_0$ . This line could be charged from the Tesla transformer secondary up to the maximum voltage of 485 kV during  $4 \mu\text{s}$  with the pulse repetition rate of 100 Hz. A stage of preliminary sharpening involves a limiting resistor  $R_0$ , a leakage inductance  $L$ , transmitting  $FL_1$  and intermediate  $FL_2$  lines, and a gas gap switch  $S_1$ . The transmitting line  $FL_1$  with variable wave impedances from 65 to  $88 \Omega$  connects the gas gap switch  $S_0$  with the line  $FL_2$ .

A BPF is assembled in the circuit with an open line which includes the lines  $FL_3$ – $FL_7$ , sharpening  $S_2$  and crowbar  $S_3$  switches, and a load  $R_L = 12.5 \Omega$ . The leakage inductance  $L$  serves to remove residual charge at the electrodes of the switches  $S_0$  and  $S_1$  by the moment of generation of the following voltage pulse. Resistor  $R_0$  allows reducing voltage oscillations in the circuit  $FL_0 - S_0 - R_0 - FL_1 - FL_4 - S_1 - S_2$  after the bipolar pulse formation and decreasing the erosion of the switch electrodes.

Figure 3 shows the design of a preliminary sharpening stage and a BPF. It consists of two gas volumes and the oil one. In the first volume, in the nitrogen atmosphere under the pressure of 85 atm, the lines  $FL_1$  and  $FL_2$ , the switch

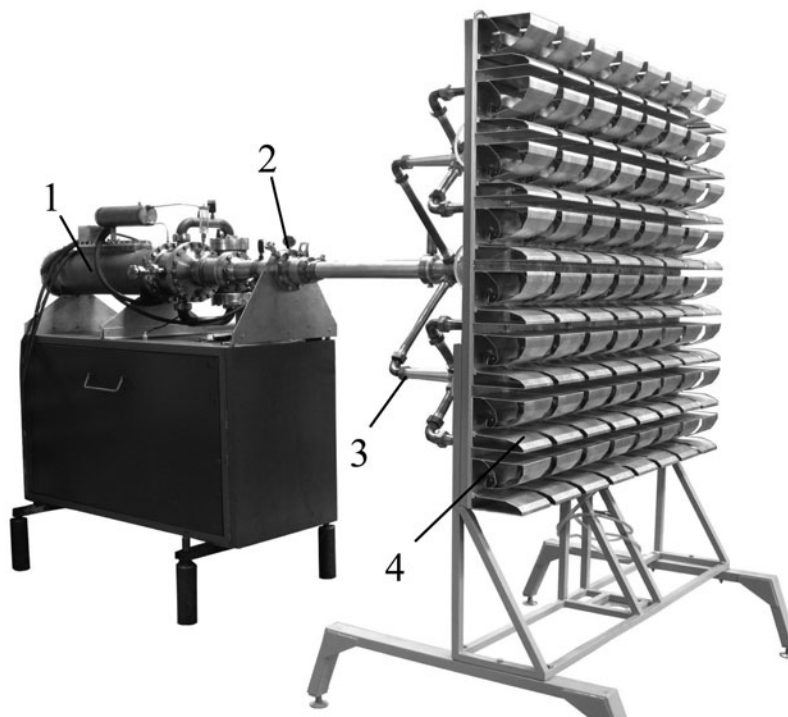


**Fig. 1.** Physical configuration of the source. (1) monopolar pulse generator, (2) bipolar pulse former, (3) power divider, (4) transmitting 64-element array.

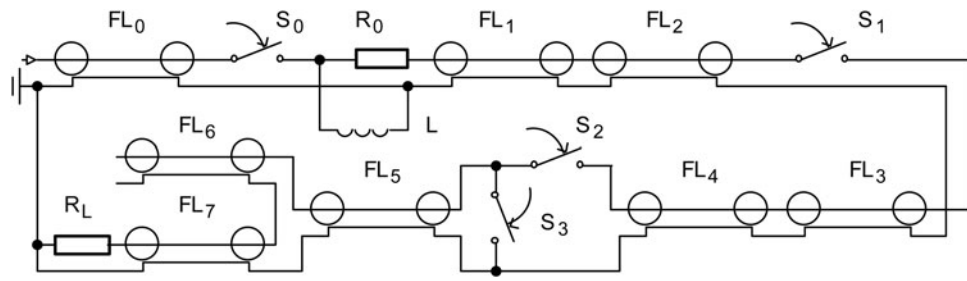


Fig. 2. Functional diagram of a bipolar pulse generator.

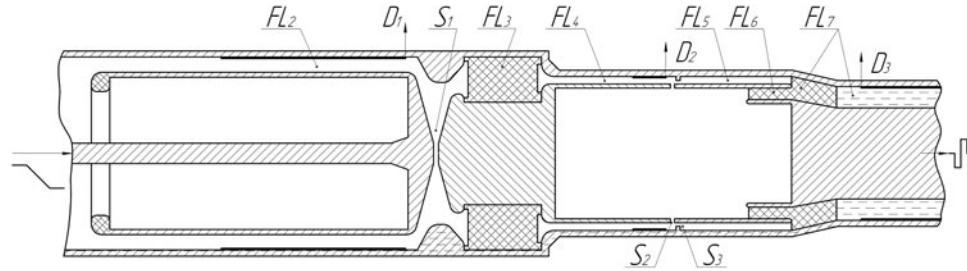


Fig. 3. Design of a preliminary sharpening stage and a bipolar pulse former.

$S_1$ , and a capacitive voltage divider  $D_1$  are placed. The line  $FL_1$  is not shown in Figure 3. Electrodes of the switch  $S_1$  are made of copper and installed with a 2.8 mm gap. In the second volume, under the nitrogen pressure of 87 atm, the lines  $FL_4$  and  $FL_5$ , a capacitive voltage divider  $D_2$ , and the switches  $S_2$ ,  $S_3$  are located. The lines  $FL_3$ ,  $FL_6$ , and the left side of the line  $FL_7$  are insulated with polyamide and serve simultaneously as the bushings. Electrodes of the switches  $S_2$  and  $S_3$  are the copper inserts at the ends of the internal conductors of the lines. The inter-electrode gaps in the switches  $S_2$  and  $S_3$  are equal to 1.7 and 1 mm, respectively. The lines  $FL_2$ ,  $FL_4$ ,  $FL_5$  have the wave impedances of 6.25  $\Omega$ .

The internal diameters of the lines  $FL_4$  and  $FL_5$  are equal to 68 mm. In contrast to the previous work (Koshelev *et al.*, 2008), where the forming line was made in the form of series-connected disk lines and switching of the lines was performed with a 15 mm diameter ring switch, in this case a coaxial line with a 68 mm diameter ring switch is used to increase the electric strength. The capacitive dividers  $D_1$  and  $D_2$  are not calibrated and serve to estimate the charging time of the intermediate  $FL_2$  and forming  $FL_4$  lines. The right side of the transmission line  $FL_7$  is an oil-filled coaxial with the wave impedance of 12.5  $\Omega$ . Inside the coaxial, a coupled-line divider  $D_3$  is installed to record an output bipolar voltage pulse by means of a 6 GHz frequency-band TDS 6604 oscilloscope. The load  $R_L$  was a water line with losses (is not shown in Fig. 3).

The charging voltage pulses entered the line  $FL_2$  from the monopolar pulse generator. After series operation of the switches  $S_1$ – $S_3$ , the output voltage pulse was removed to the load  $R_L$  through the transmission line  $FL_7$ . The adjustment of the bipolar voltage pulse generator consisted in the

series setting of the gaps and pressures in the switches  $S_1$ – $S_3$ . The delay time of operation of the sharpening switches  $S_1$  and  $S_2$  was chosen so that their breakdown occurred near the maximum charging voltage of the lines  $FL_2$  and  $FL_4$ , without misses at a pulse repetition rate of 100 Hz. Then, a symmetrical waveform of the output bipolar pulse was achieved by adjusting the gap in the crowbar switch  $S_3$ . Thus, the delay time of breakdown of the switches  $S_1$  and  $S_2$  was 7.3 and 1.7 ns, respectively.

The output bipolar voltage pulse recorded from the divider  $D_3$  and presented in Figure 4 has the voltage amplitudes of –205 kV and +180 kV and the length  $\tau_p = 1$  ns at the level of 0.1 of the amplitudes. A root-mean-square deviation of the voltage amplitude is no higher than 4%. The pulse energy absorbed by the matched load of 12.5  $\Omega$  is equal to 1.2 J that is 9% of the energy stored in the forming line  $FL_0$ .

Due to a high rate of the voltage rise at the electrodes of the switches  $S_2$  and  $S_3$ , a multichannel commutation of the lines with the wave impedance of 6.25  $\Omega$  by means of the 68 mm diameter ring switches was obtained. In comparison with the previous work (Koshelev *et al.*, 2008), the rate of the negative voltage rise at the BPF output increased by a factor of 1.4.

#### 4. POWER DIVIDER

To transmit a bipolar voltage pulse from the generator to the antenna array elements, a previously designed (Koshelev *et al.*, 2010) 64-channel power divider with simultaneous impedance conversion is used. Structurally, the 64-channel power divider consists of three series-connected stages of four-channel dividers. At the input of the first stage, the wave impedance equals to the one of a 12.5  $\Omega$  bipolar

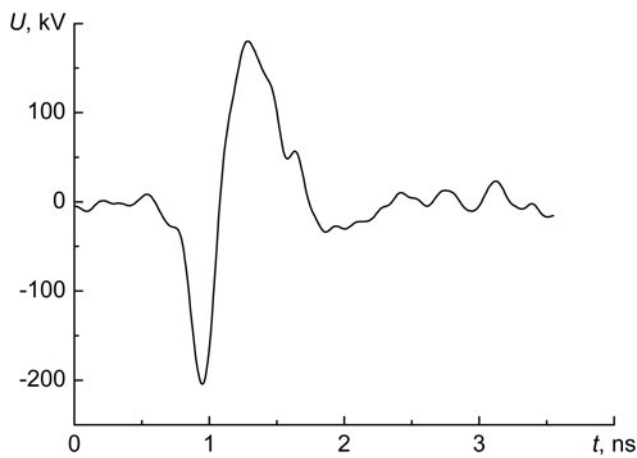


Fig. 4. Output voltage pulse waveform.

pulse generator at its output. At the initial part of the arm of the divider first stage, the wave impedance is  $12.5 \times 4 = 50 \Omega$ . The total impedance of the feeders of 16 array elements, which is loaded by each arm of the first stage, equals to  $50/16 = 3.125 \Omega$ , while the total impedance of the feeders of 64 array elements equals to  $50/64 \approx 0.78 \Omega$ . A compensated exponential junction was used for the impedance conversion. The total length of one arm of the divider is 1.2 m.

In the previous works (Koshelev *et al.*, 2008; 2010), the transformer oil was used as an insulator for the feeder system. Due to the great losses in the transformer oil, the feeder system lost up to 50% of the power. Romanchenko *et al.* (2012) have shown that using the vacuum oil instead of the transformer one results in a reduction of power losses. Low-voltage tests of the feeder system of a 64-element antenna array have shown that using the BM-1 vacuum oil allows decreasing power losses up to 30%. Figure 5 presents the waveforms of the voltage pulses at

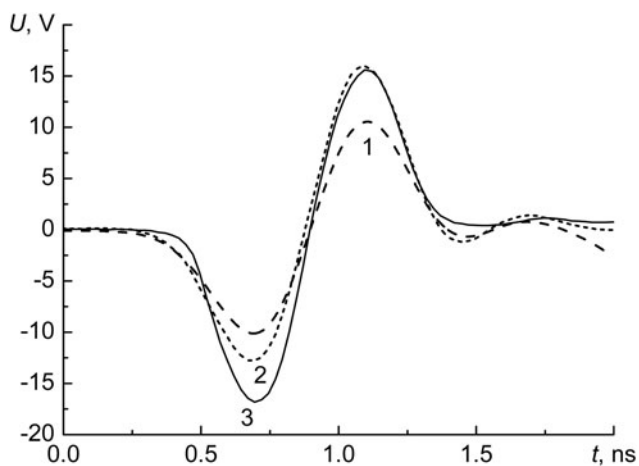


Fig. 5. Voltage pulse waveforms from one of the outputs of a 64-channel power divider when using the transformer (1), the vacuum (2) oils and in the absence of power losses (3).

the output of the feeder system of a 64-element array when using the transformer (curve 1) and the vacuum (curve 2) oils. For comparison, a voltage pulse waveform in the assumption of absence of the losses is presented (curve 3).

## 5. RADIATION OF ULTRAWIDEBAND PULSES

The array was excited with a high-voltage pulse presented in Figure 4. Radiated pulse was recorded by means of a TEM-horn mounted at a 10.5 m distance in the pattern maximum using a LeCroy WaveMaster 830Zi oscilloscope with the frequency band of 30 GHz. Figure 6 shows the waveform of the radiated pulse. Due to the features of the room in which the measurements were carried out, after a dashed line the pulse is superimposed by the reflections from the surrounding metal objects. In these measurements, the product of the peak field strength by the distance reached 4.1 MV.

In order to determine the effective potential of radiation, it is necessary to define the far-field zone boundary. For this purpose, we will use the relation for the harmonic signals  $r = 2D^2/\lambda_0$ , where  $\lambda_0 = \tau_p c$ ,  $\tau_p$  is the length of a bipolar voltage pulse at the input of the feeder system,  $c$  is the velocity of light,  $D$  is the maximum transverse dimension of the antenna array. Previous researches (Gubanov *et al.*, 2005; Efremov *et al.*, 2011) have shown the validity of using this relation for estimation of the far-field zone boundary at excitation of the antenna arrays with bipolar pulses. This estimation of the position of the far-field zone boundary corresponded to the criteria  $rE_p \approx const$  used in the measurements. This is caused by the fact that the energy of the radiated UWB pulse is concentrated near the central frequency with the wavelength  $\lambda_0$ . The position of the far-field zone boundary for a 64-element antenna array excited with a bipolar voltage pulse of the length  $\tau_p = 1$  ns according to the foregoing relation is  $r = 26.7$  m. Since measurements of  $rE_p$  for a 64-element antenna array were carried out at a distance of 10.5 m, then basing on the previously performed research of a  $4 \times 4$  array excited with a bipolar pulse of the length 2 ns (Gubanov *et al.*, 2005), where the criterion  $rE_p \approx$

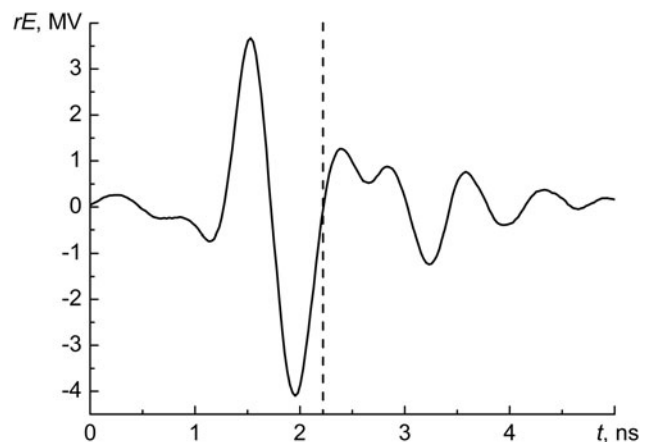


Fig. 6. Waveform of the pulse radiated by a 64-element array.

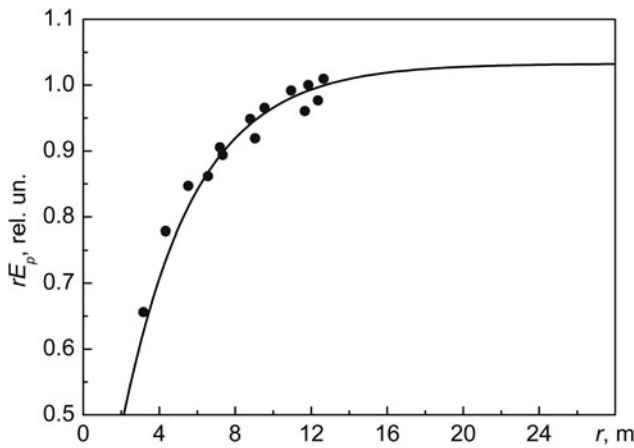


Fig. 7. Value  $rE_p$  versus distance.

*const* was realized, the extrapolation of the  $rE_p(r)$  dependence was tracked for a 64-element antenna array up to the boundary of the far-field zone (Fig. 7). In this figure, the points show the previously received measurement results for the 64-element array (Koshelev *et al.*, 2008; 2010). From these data it follows that the effective potential of radiation  $rE_p$  determined in the far-field zone is 5.8% higher than the value  $rE_p(r = 10.5 \text{ m})$  making up 4.3 MV.

The stability and the operating time of the source of UWB radiation has been tested at a pulse repetition rate of 100 Hz (Fig. 8). Every 10 minutes of continuous operation were followed by an hour interruption to cool the BPF. At the beginning of the series, the nitrogen pressure in the switches was of 84–86 atm and after 10 minutes of operation it rises by 2 atm. With that, the value of  $rE_p$  decreased by 20%. The bipolar voltage amplitudes reduce as well but the pulse length had no changes. Cooling of the BPF resulted in no full restoration of the initial value  $rE_p = 4.1 \text{ MV}$ . A root-mean-square deviation  $\sigma$  of the value  $rE_p$  was significant at the beginning of ten-minute pulse trains and decreased to the value of ~3%.

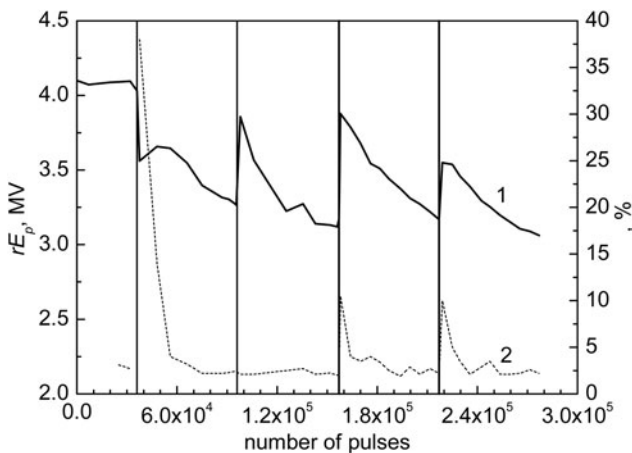


Fig. 8. Effective potential of radiation (1) and its root-mean-square deviation (2) versus the number of pulses.

For a long-term continuous operation with small changes in the value  $rE_p$ , it is necessary to use forced cooling of the BPF and pressure adjustment in the switches, which is the subject of further research.

### 6. DISCUSSION

To compare two developing directions of high-power UWB sources, it was interesting to use the relation proposed by Belichenko *et al.* (2006) to estimate the limiting effective potential of radiation of an arbitrary antenna

$$rE_{\theta} = \frac{\sqrt{Z_0 W}}{2\sqrt{2\pi}} \sqrt{\int_{\Omega} \left[ \sum_{n=1}^{N(\omega)} (2n + 1) \right] d\omega}.$$

Here  $Z_0$  is the free-space wave impedance,  $W$  is the pulse energy at the antenna input radiated with a 100% efficiency,  $N = [\omega_0 a / c + 2\pi]$ ,  $\omega_0$  is the central cyclic frequency of radiation spectrum,  $2\Delta\omega$  is the radiation spectrum width determined by the level of -10 dB,  $\Omega = \{\omega_0 - \Delta\omega < \omega < \omega_0 + \Delta\omega\}$  is the integration region,  $a$  is the radius of an imaginary sphere inside which a radiator is located.

To make a comparative analysis of various radiators, we will use an efficiency factor determined as the ratio of the experimentally measured potential to the limiting one:  $k = rE_{exp} / rE_{\theta}$ . As it follows from the data presented in Figure 9, a single CA ( $k = 0.26$ ) (Gubanov *et al.*, 2005) is significantly less effective than a 3.66 m diameter impulse radiating antenna ( $k = 0.5$ ) (Giri *et al.*, 1997). For a 16-element array CA (Gubanov *et al.*, 2005), the efficiency factor  $k = 0.58$ , while for a 64-element array CA,  $k = 0.65$  at a maximum transverse dimension  $D = 2 \text{ m}$ . Hence, as it follows from the data presented above, the efficiency of the radiator increases with the rise of the number of elements in the array despite the energy losses in the feeder system.

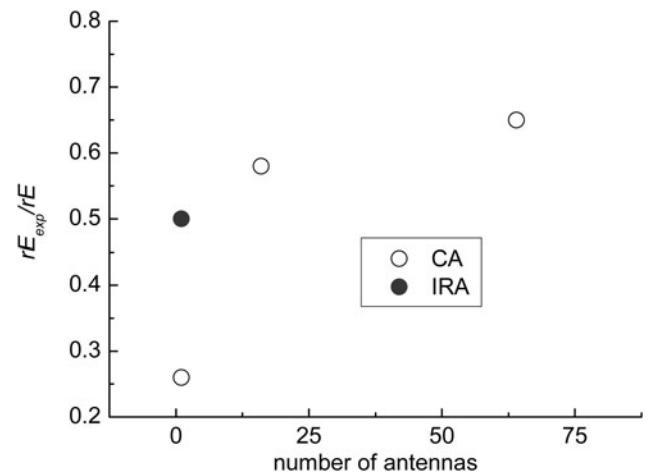


Fig. 9. Measured effective potential of radiation versus the limiting one for various radiators.

To estimate UWB radiators, an efficiency factor by the peak field strength is used widely which is determined as the ratio of the effective potential of radiation to the voltage pulse amplitude at the antenna input  $k_E = rE_p / \{U_{\max}\}$ . For the UWB source with a 64-element array,  $k_E = 21$  while for the JOLT source (Baum et al., 2004)  $k_E = 6$ .

From a foregoing brief analysis it follows that the UWB sources based on multi-element arrays have higher efficiency in several parameters than the sources based on impulse radiating antenna. This is due to the fact that compact combined antennas excited with a bipolar voltage pulse are used in the arrays. It should be noted that the energy radiated is also higher which is caused by the longer duration of the pulse.

## 7. CONCLUSION

As a result of the work performed, a new design of a bipolar pulse former has been developed providing a stable operation of the voltage pulse generator with the wave impedance of 12.5  $\Omega$  and amplitude of 200 kV at a 100 Hz frequency. Energetic efficiency of the feeder system was increased from 50% to 70% due to reduction of the losses in a liquid dielectric. UWB radiation pulses with the effective potential of up to 4.3 MV were obtained in the experiments. Continuous operation of the source was 10 minutes and it was limited due to the heating of the bipolar pulse former.

## REFERENCES

- AGEE, F.J., BAUM, C.E., PRATHER, W.D., LEHR, J.M., O'LOUGHLIN, J.P., BURGER, J.W., SCHOENBERG, J.S.H., SCHOLFIELD, D.W., TORRES, R.J., HULL, J.P. & GAUDET, J.A. (1998). Ultra-wideband transmitter research. *IEEE Trans. Plasma Sci.* **26**, 860–873.
- ANDREEV, YU.A., GUBANOV, V.P., EFREMOV, A.M., KOSHELEV, V.I., KOROVIN, S.D., KOVALCHUK, B.M., KREMNEV, V.V., PLISKO, V.V., STEPCHENKO, A.S. & SUKHUSHIN, K.N. (2003). High-power ultrawideband radiation source. *Laser Part. Beams* **21**, 211–217.
- ANDREEV, YU.A., BUYANOV, YU.I. & KOSHELEV, V.I. (2005). A combined antenna with extended bandwidth. *J. Commun. Technol. Electron.* **50**, 535–543.
- ANDREEV, YU.A., EFREMOV, A.M., KOSHELEV, V.I., KOVALCHUK, B.M., PLISKO, V.V. & SUKHUSHIN, K.N. (2011). Generation and emission of high-power ultrabroadband picosecond pulses. *J. Commun. Technol. Electron.* **56**, 1429–1439.
- BAUM, C.E. & FARR, E.G. (1993). Impulse radiating antennas. In *Ultra-Wideband, Short-Pulse Electromagnetics* (Bertoni, H.L., Carin, L., & Felsen, L.B., Eds.), pp. 139–147. New York: Plenum Press.
- BAUM, C.E., BAKER, W.L., PRATHER, W.D., LEHR, J.M., O'LOUGHLIN, J.P., GIRI, D.V., SMITH, I.D., ALTES, R., FOCKLER, J., McMILLAN, D., ABDALLA, M.D. & SKIPPER, M.C. (2004). JOLT: A highly directive, very intensive, impulse-like radiator. *Proc. IEEE.* **92**, 1096–1109.
- BELICHENKO, V.P., KOSHELEV, V.I., PLISKO, V.V., BUYANOV, YU.I. & LITVINOV, S.N. (2006). Estimation of an utmost efficient potential of ultrawideband radiating system. In *the Proceedings of the 14 International Symposium of High Current Electronics*. pp. 391–394. Tomsk, Russia.
- EFREMOV, A.M., KOSHELEV, V.I., KOVALCHUK, B.M., PLISKO, V.V. & SUKHUSHIN, K.N. (2007). Generation and radiation of high-power ultrawideband nanosecond pulses. *J. Commun. Technol. Electron.* **52**, 756–764.
- EFREMOV, A.M., KOSHELEV, V.I., KOVALCHUK, B.M., PLISKO, V.V. & SUKHUSHIN, K.N. (2011). High-power sources of ultra-wideband radiation with subnanosecond pulse lengths. *Instrum. Exp. Tech.* **54**, 70–76.
- GIRI, D.V., LACKNER, H., SMITH, I.D., MORTON, D.W., BAUM, C.E., MAREK, J.R., PRATHER, W.D. & SCHOLFIELD, D.W. (1997). Design, fabrication, and testing of a paraboloidal reflector antenna and pulser system for impulse-like waveforms. *IEEE Trans. Plasma Sci.* **25**, 318–326.
- GUBANOV, V.P., EFREMOV, A.M., KOSHELEV, V.I., KOVALCHUK, B.M., KOROVIN, S.D., PLISKO, V.V., STEPCHENKO, A.S. & SUKHUSHIN, K.N. (2005). Sources of high-power ultrawideband radiation pulses with single antenna and a multielement array. *Instrum. Exp. Tech.* **48**, 312–320.
- KOSHELEV, V.I., BUYANOV, YU.I., KOVALCHUK, B.M., ANDREEV, YU.A., BELICHENKO, V.P., EFREMOV, A.M., PLISKO, V.V., SUKHUSHIN, K.N., VIZIR, V.A. & ZORIN, V.B. (1997). High-power ultrawideband electromagnetic pulse radiation. *SPIE* **3158**, 209–219.
- KOSHELEV, V.I., BUYANOV, YU.I., ANDREEV, YU.A., PLISKO, V.V. & SUKHUSHIN, K.N. (2001). Ultrawideband radiators of high-power pulses. *IEEE* **2**, 1661–1664.
- KOSHELEV, V.I., EFREMOV, A.M., KOVALCHUK, B.M., PLISKO, V.V. & SUKHUSHIN, K.N. (2008). High-power source of ultrawideband radiation wave beams with high directivity. In *the Proceedings of the IEEE International Pulsed Power Plasma Science Conference*, **2**, pp. 1661–1664. Las Vegas, Nevada.
- KOSHELEV, V.I., PLISKO, V.V. & SUKHUSHIN, K.N. (2010). Array antenna for directed radiation of high-power ultra-wideband pulses. In *Ultra-Wideband, Short-Pulse Electromagnetics 9* (Sabath, F., Giri, D.V., Rachidi, F., Kaelin, A., Eds.), pp. 259–267. New York: Springer.
- MESYATS, G.A., KOROVIN, S.D., GUNIN, A.A., GUBANOV, V.P., STEPCHENKO, A.S., GRISHIN, A.V., LANDL, V.F. & ALEKSEENKO, P.I. (2003). Repetitively pulsed high-current accelerators with transformer charging of forming lines. *Laser Part. Beams* **21**, 197–209.
- ROMANCHENKO, I.V., ROSTOV, V.V., GUBANOV, V.P., STEPCHENKO, A.S., GUNIN, A.V. & KURKAN, I.K. (2012). Repetitive sub-gigawatt rf source based on gyromagnetic nonlinear transmission line. *Rev. Sci. Instrum.* **83**, 074705.
- SABATH, F., NITSCH, D., JUNG, M. & WEISE, T.H.G.G. (2002). Design and setup of a short pulse simulator for susceptibility investigations. *IEEE Trans. Plasma Sci.* **30**, 1722–1727.